

Cross-Linking of Poly(vinyl alcohol) Chains by Al Ions in Macro-Defect-Free Cements: A Theoretical Study

Aldo Amore Bonapasta*

Consiglio Nazionale delle Ricerche—Istituto di Chimica dei Materiali (ICMAT),
V. Salaria Km. 29,5—CP 10, 00016 Monterotondo Scalo, Italy

Francesco Buda

Department of Physical and Theoretical Chemistry, Vrije Universiteit Amsterdam De
Boelelaan 1083, NL-1081 HV Amsterdam, The Netherlands

Pierre Colombet

CTG-Italcementi Group, Via Camozzi 124—24121 Bergamo, Italy

Received July 27, 1999. Revised Manuscript Received December 7, 1999

The significant increases in flexural strength achieved in macro-defect-free cements have been attributed to a reduction in the density of defects in the materials as well as to chemical reactions occurring between the organic constituent, i.e., the poly(vinyl alcohol) (PVA) polymer, and inorganic ions coming from the hydration products of the cement. In particular, it has been suggested that PVA chains are partially linked together by Al ions. This phenomenon has been investigated here by studying the structure and the energetics of Al–PVA models with *ab initio* theoretical methods. The achieved results strongly support the existence of a cross-linking of PVA chains by Al ions, even in the presence of structural deformations of the PVA chains. The vibrational frequency of a stretching mode related to the O atoms bonded with Al has been also evaluated, which may represent a fingerprint for an experimental identification of cross-linking.

Introduction

Macro-defect-free (MDF) cements were originally proposed by Birchall and co-workers as a new class of composite materials having unique mechanical properties.^{1,2} A major characteristic of these materials is represented by a flexural strength which is more than 150 MPa as compared to values of the order of 10 MPa for conventional cement pastes.^{3–5} Furthermore, the MDF paste has a workable viscosity, so that MDF materials may be considered as a type of “inorganic plastic”. The term MDF refers to the absence of the relatively large voids or defects which are usually present in cement pastes.^{1,3,4} The density of defects is successfully reduced by mixing a cement powder with a water-soluble polymer and a minimal amount of water under high shear and subsequent molding under pressure at 80 °C.^{3,5} The best mechanical properties for MDF materials have been achieved by mixing high-alumina cements and poly(vinyl alcohol)-poly(vinyl acetate) (PVAc). The anhydrous components of these cements are

calcium aluminates, mainly CaAl_2O_4 and CaAl_4O_7 , which give rise to MDF materials whose mineral composition corresponds to a 70% and a 29% of Al_2O_3 and CaO by weight, respectively. Portland cements—whose main components are calcium silicates, Ca_3SiO_5 —and PVAc may be also used to obtain MDF materials with 6% and 67% of Al_2O_3 and CaO by weight, respectively. However, Portland MDF cements do not reach the high flexural strengths characterizing the high-alumina cements.³

The polymer used in the realization of the MDF cements was initially considered only as a rheological aid facilitating particle packing as well as a filling agent reducing the material porosity.² However, studies on the chemistry and the microstructure of the calcium aluminate MDF materials have attributed the significant improvements of the mechanical properties of these materials also to the chemical reactions occurring between the PVA polymer (the poly(vinyl alcohol) arising from the PVAc hydrolysis) and the inorganic ions produced when the cement constituents dissolve in water.^{3–9} The microstructure of calcium aluminate MDF materials and the chemical interaction of the organic

* To whom correspondence should be addressed.

(1) Birchall, J. D.; Howard, A. J.; Kendall, K. *Nature* **1981**, *289*, 388–389.

(2) Kendall, K.; Birchall, J. D. *Mater. Res. Soc. Symp. Proc.* **1985**, *42*, 143–150.

(3) Berg, M.; Young, J. F. *Mater. Res. Soc. Symp. Proc.* **1992**, *271*, 609.

(4) Roy, D. M. *9th Int. Congr. Chem. Cem.* [New Delhi (India)] **1992**, *1*, 357.

(5) Lewis, A. J.; Kriven, M. W. *MRS Bull.* **1993** (March), 72.

(6) Rodger, S. A.; Sinclair, W.; Groves, G. W.; Brooks, S. A.; Double, D. D. *J. Mater. Sci.* **1985**, *20*, 2853.

(7) Rodger, S. A.; Sinclair, W.; Groves, G. W.; Brooks, S. A.; Double, D. D. *Mater. Res. Symp. Proc.* **1985**, *42*, 45.

(8) Popoola, O. O.; Kriven, W. M.; Young, J. F. *J. Am. Ceram. Soc.* **1991**, *74*, 1928.

(9) Popoola, O. O.; Kriven, W. M. *J. Mater. Res.* **1992**, *7*, 1545.

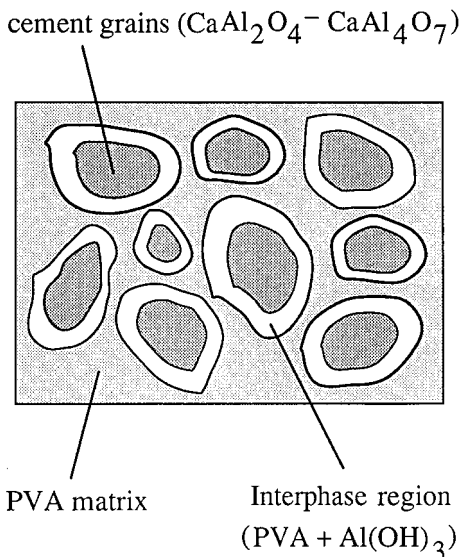


Figure 1. Schematic view of the microstructure of a calcium aluminate MDF cement.

components with the inorganic ones have been investigated by transmission (TEM) and scanning (SEM) electron microscopies,^{8,9} X-ray photoelectron spectroscopy (XPS),⁹⁻¹² infrared spectroscopy (IR)^{10,11} and differential thermal analysis (DTA).¹¹ The main results of those experimental studies are summarized as follows. The microstructure of MDF materials is characterized by grains of partially hydrated calcium aluminates embedded in a matrix of PVA polymer, as illustrated in Figure 1. Interphase regions coat individual cement grains. These regions consist of an amorphous phase of $\text{Al}(\text{OH})_3$ and PVA inside of which are dispersed fine crystallites of hydration products. These interphase regions influence the properties of the MDF materials. In particular, it has been shown that the mechanical behavior of the interphase regions plays an important role during the fracture of the MDF materials.^{13,14} The presence of aluminum and PVA chains in the interphase regions and an analogy with the behavior of boron with PVA led to the suggestion of the existence of a cross-linking of the PVA chains by Al ions,^{6,7} i.e., the formation of O–Al–O bonds where Al is bonded to the O atoms of two different PVA chains. Polycondensation reactions such as those shown in Figure 2 were proposed for aluminum, by analogy with the case of boron. Cross-linking can strengthen the network of the PVA chains around the cement grains, therefore, its existence may provide a basis for understanding the relationships between the microstructure and the mechanical properties of the MDF materials.^{15,16} Moreover, a chemical effect, like cross-linking, may account for the achievement of mechanical properties in the composite MDF materials which are better than

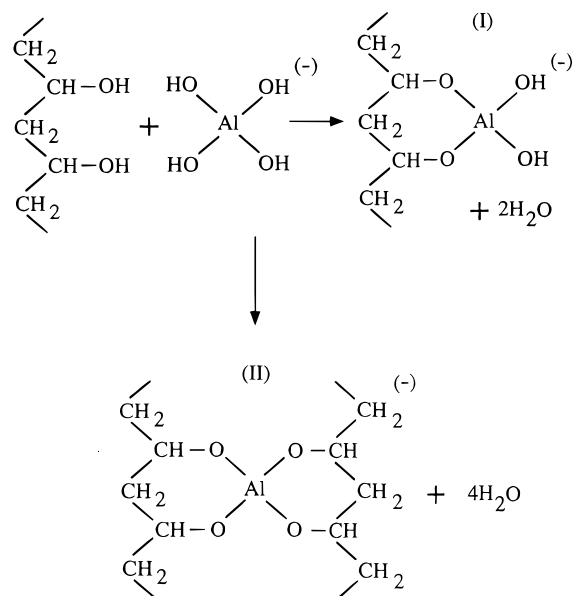


Figure 2. Polycondensation reactions involving PVA chains and the $\text{Al}(\text{OH})_4^-$ complex. One and two PVA chains are involved in the formation of the Al–PVA systems I and II, respectively.

those of the individual components, as shown, e.g., by a comparison of the bending strengths of the ordinary cement, the PVA polymer and the MDF cements which are equal to 10,⁵ 70,¹⁷ and 150 MPa,⁴ respectively.

Despite its potential and interesting effects, only indirect evidence of cross-linking has been found experimentally.^{8,9,11} Furthermore, experimental investigations were not able to distinguish between the configurations I and II in Figure 2. Finally, doubts on the cross-linking of PVA by Al ions have been raised by a study performed on dilute and semidilute solutions of PVA mixed with aluminate or borate solutions which has shown the formation of a gel (i.e., a cross-linking effect) only in the latter case.¹⁸

The above arguments and the uncertainties of the experimental results have motivated the present study where the cross-linking of PVA chains by Al ions has been investigated by ab initio theoretical methods. It has been assumed here that the reaction of calcium aluminates with water leads to the formation of $\text{Al}(\text{OH})_4^-$ molecules which are involved in the polycondensation reactions shown in Figure 2. The Car–Parrinello method^{19,20} has been used to estimate the energies released in these reactions as well as to investigate the equilibrium geometries, the electronic charge distributions, and the chemical bonding of several model systems where an Al ion is tetrahedrally coordinated with four O atoms. In these systems, the Al^{3+} ion is bonded with zero, one, and two PVA chains (see the structures of the $\text{Al}(\text{OH})_4^-$ molecule and of the Al–PVA-(I) and Al–PVA(II) models shown in parts a, b and c of Figure 3, respectively). The strength of the Al–O bonds has been investigated both for the equilibrium geometry

(10) Shuguang Hu **1992**, 3, 393.

(11) Harsh, S.; Naidu, Y. C.; Ghosh, S. N. *9th Int. Congr. Chem. Cem.* [New Delhi (India)] **1992**, 3, 406.

(12) Shuguang Hu *Cem. Concr. Res.* **1994**, 24, 1509.

(13) Cannon, M. C.; Groves, G. W. *J. Mater. Sci.* **1986**, 21, 4009.

(14) Poon, C. S.; Wassel, L. E.; Groves, G. W. *Mater. Sci. Technol.* **1988**, 4, 993.

(15) Gulgun, M. A.; Kriven, W. M.; Tan, L. S.; McHugh, A. J. *J. Mater. Res.* **1995**, 10, 1746.

(16) Tan, L. S.; McHugh, A. J.; Gulgun, M. A.; Kriven, W. M. *J. Mater. Res.* **1996**, 11, 1739.

(17) Finch, C. A. *Polyvinyl Alcohol Developments*; John Wiley & Sons Ltd: New York, 1992.

(18) Desai, P. G.; Young, J. F.; Wool, R. P. *Mater. Res. Soc. Symp. Proc.* **1992**, 245, 179.

(19) Car, R.; Parrinello, M. *Phys. Rev. Lett.* **1985**, 55, 2471.

(20) Galli, G.; Pasquarello, A. *Computer Simulation in Chemical Physics*; Allen M. P., Tildsley, D. J., Eds.; Kluwer: Amsterdam, 1993.

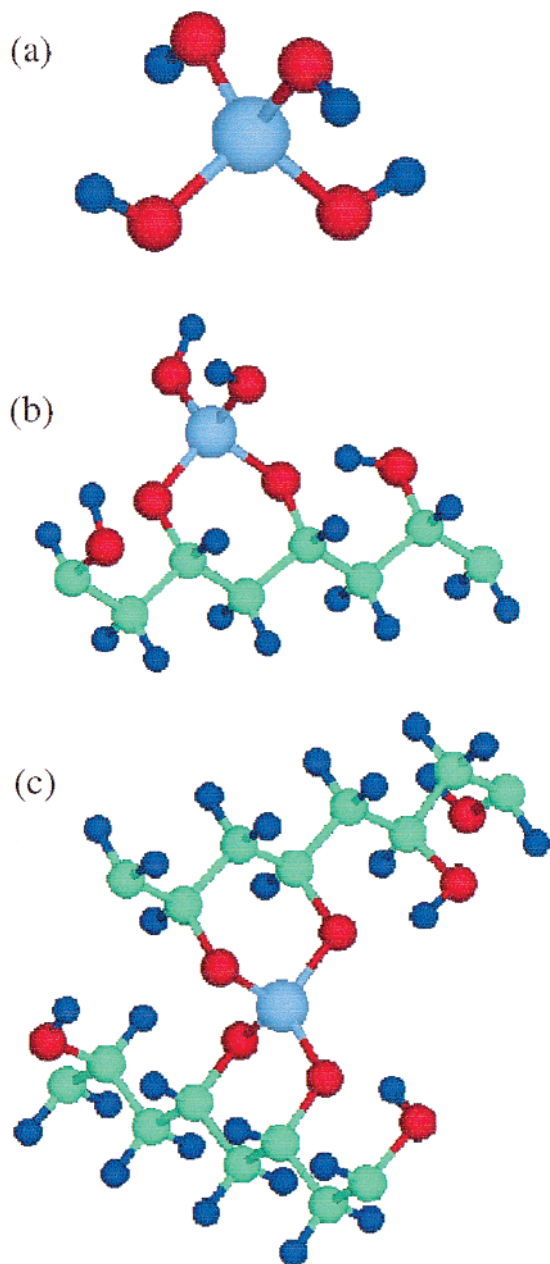


Figure 3. (a) Structure of the $\text{Al}(\text{OH})_4^-$ complex; (b) structure of the Al–PVA(I) system (see text and Figure 2); and (c) structure of the Al–PVA(II) system (see text and Figure 2). In the Al–PVA(II) system a cross-linking is realized by an Al ion tetrahedrally coordinated with four O atoms of two PVA chains. In the calculations, the fragments of the PVA chains shown in the figure are repeated along the chain axis to simulate chains of infinite length. The Al, C, O, and H atoms are identified by the colors cyan, green, red, and blue, respectively.

and for distorted geometries of the Al–PVA(I) model to evaluate the effects of deformations of the PVA chains on the stability of cross-linking. Present results strongly support the existence of cross-linking of PVA chains by Al ions. Furthermore, they predict a Raman-active vibrational frequency which is related to the formation of the AlO_4 fragment characterizing the Al–PVA model shown in Figure 3c. This vibrational frequency could be used as a fingerprint to achieve experimental evidences of cross-linking.

Computational Methods

In the Car–Parrinello (CP) method, the interatomic forces are computed from the instantaneous quantum-mechanical electronic ground state in the Born–Oppenheimer approximation. The electronic ground state corresponding to a given atomic geometry is obtained within the density-functional theory (DFT).^{21,22} The exchange–correlation functional used in the calculations includes gradient corrections (GC) to the local density approximation (LDA)^{23,24} in the form proposed by Becke and Perdew.^{25,26} Only the valence electrons are taken into account while the atomic inner cores are frozen. The interaction between the valence electrons and the frozen cores is described by soft first-principle pseudopotentials.²⁷ The single-particle Kohn–Sham wave functions are expanded on a plane wave basis set, thus implying the use of periodic boundary conditions (PBC). In the present calculations, the PBC have been applied to a supercell (i.e., the simulation box) containing a fragment of the PVA chain aligned with one side of the cell. This approach allows us to describe a PVA chain as a system with full translational periodicity in one dimension. The sides of the simulation box (10.06, 10.06, and 6.94 Å) are chosen to contain two PVA chains arranged as in Figure 3c. These supercell sizes also minimize possible, spurious interactions between the fragments in the supercell and their images. CP calculations have been successfully performed in the investigation of structural and electronic properties of complex organic molecules.^{28,29} Notwithstanding, further tests have been performed here to verify the convergence of the calculations with respect to the kinetic energy cutoff (which controls the number of plane waves used in the calculations) as well as to check the methods in the cases of simple molecules. As far as the kinetic energy cutoff is concerned, convergence has been achieved by using a value of 22 Ry, in agreement with the results of previous studies.³⁰ Equilibrium geometries (i.e., bond angles and bond lengths) have been evaluated in the cases of the CH_4 , Al–O, and $\text{Al}(\text{OH})_4^-$ molecules and of an isolated PVA chain. In the CH_4 and PVA cases, a tetrahedral symmetry has been found around the C atoms, the values of 1.10, 1.51, 0.99, and 1.44 Å have been calculated for the C–H, C–C, O–H, and C–O bond lengths, respectively, in good agreement with experimental values.³¹ In the $\text{Al}(\text{OH})_4^-$ molecule, a tetrahedral symmetry has been found around the Al atoms. Values of 1.70 and 1.73 Å have been calculated for the Al–O bond lengths in the Al–O and $\text{Al}(\text{OH})_4^-$ molecules, respectively, in good agreement with the value of 1.75 Å measured in sodalite.³² The harmonic approximation has been used to evaluate the stretching frequencies of the C–H bond in the CH_4 molecule and of the C–H, C–O, and O–H in the PVA chain. The vibrational frequency estimated in the first case, 2861 cm^{-1} , is in quite good agreement with the experimental one, 2951 cm^{-1} .³³ The frequencies calculated for the PVA chain are also in agreement with experiment as will be discussed in the next section. Finally, the dissociation energy of the diatomic molecule Al–O has been estimated. A theoretical value of 6.6 eV has been given by the difference of the total energies (E) calculated for

(21) Parr, R. G.; Yang, W. *Density Functional Theory of Atoms and Molecules*; Oxford University Press: New York, 1989.

(22) Jones, R. O.; Gunnarson, O. *Rev. Mod. Phys.* **1989**, *61*, 689.

(23) Perdew, J. P.; Zunger, A. *Phys. Rev. B* **1981**, *23*, 5048.

(24) Ceperley, D. M.; Alder, B. J. *Phys. Rev. Lett.* **1980**, *45*, 566.

(25) Becke, A. D. *Phys. Rev. A* **1988**, *38*, 3098.

(26) Perdew, J. P. *Phys. Rev. B* **1986**, *33*, 8822.

(27) Vanderbilt, D. *Phys. Rev. B* **1990**, *43*, 7892.

(28) Buda, F.; de Groot, H. J. M.; Bifone, A. *Phys. Rev. Lett.* **1996**, *77*, 4474.

(29) La Penna, G.; Buda, F.; Bifone, A.; de Groot, H. J. M. *Chem. Phys. Lett.* **1998**, *294*, 447.

(30) Bifone, A.; de Groot, H. J. M.; Buda, F. *J. Phys. Chem. B* **1997**, *101*, 2954.

(31) *CRC Handbook of Chemistry and Physics*; Weast R. C., Lide, D. R., Eds.; CRC Press: Boca Raton, FL, 1989.

(32) Trave, A.; Buda, F.; Selloni, A. *J. Phys. Chem. B* **1998**, *102*, 1522.

(33) Herzberg, G. *Infrared and Raman spectra*; Van Nostrand Reinhold Company: New York, 1945.

Table 1. Calculated Bond Lengths (in angstroms) for the Optimized Structures of the Three Systems Investigated Here (see the text) (Experimental estimates of some bond lengths are given in the last column)

bonds	systems			exp
	$\text{Al}(\text{OH})_4^-$	$(\text{R}-\text{CHO})_2\text{Al}(\text{OH})_2^-$	$2(\text{R}-\text{CHO})_2\text{Al}^-$	
Al–O	1.73	1.73	1.71	1.75 ^a
O–H	0.98	0.98		
C–C		1.52	1.52	1.54 ^b
C–H		1.11	1.11	1.10 ^b
C–O		1.44	1.44	1.43 ^b
O–H		1.00	0.99	0.96 ^b

^a From ref 32. ^b From ref 31.

the molecule and the constituent atoms: $E[\text{Al}-\text{O}] - (E[\text{Al}] + E[\text{O}])$. The theoretical estimate is in satisfactory agreement with the experimental value of 5.0 eV.³⁴

Results and Discussion

The existence of a cross-linking of PVA chains by Al ions is closely related to the stability of the four Al–O chemical bonds which can be formed by an Al atom and by two pairs of O atoms provided by two polymer chains (see Figure 3c). Thus, the structure and the energetics of the AlO_4 atomic arrangement have been carefully investigated here in the three different systems shown in Figure 3, all containing an Al atom tetrahedrally bonded to four O atoms. The Al–PVA(I) and Al–PVA(II) systems will be also designated as $(\text{R}-\text{CHO})_2\text{Al}(\text{OH})_2^-$ and $(2(\text{R}-\text{CHO})_2)\text{Al}^-$, respectively, to have a direct relationship with the configurations I and II of Figure 2. Within this convention, a fragment of the PVA chain will be designated as $(\text{R}-\text{CHOH})_2$. First, the equilibrium geometries of the above three systems will be discussed (see Table 1). All the calculated bond lengths are in good agreement with the experimental values measured in various solid and molecular systems. The calculated bond angles (not reported in Table 1) show a tetrahedral symmetry around the C and Al atoms in agreement with the experimental findings. Small deviations from the perfect tetrahedral angle have been found only in the case of the Al atom bonded with the PVA chains. Thus, the results reported in Table 1 show that the AlO_4 fragment has almost identical geometries in the $\text{Al}(\text{OH})_4^-$ complex and in both the Al–PVA systems. An analysis of the chemical bonding in the Al–O–C bonds related to the PVA cross-linking was then performed by evaluating isosurfaces corresponding to the same value of the valence electronic charge density. The isosurfaces corresponding to the $\text{Al}(\text{OH})_4^-$ complex and to the Al–PVA(I) and Al–PVA(II) systems are shown in parts a, b, and c of Figure 4, respectively. In the case of the $\text{Al}(\text{OH})_4^-$ complex, the strong ionic character of the Al–O bonds is clearly shown by a piling up of the electronic charge density on the O atoms (see Figure 4a). In the same figure, a polarization of the O–H bond is shown by the piling up of the charge density on the oxygen atom. In the cases of the two Al–PVA systems, the charge density distributions of parts b and c of Figure 4 clearly show the covalent character of the C–C, C–O, and C–H bonds. In the same figures, the charge density distribution around the Al atom

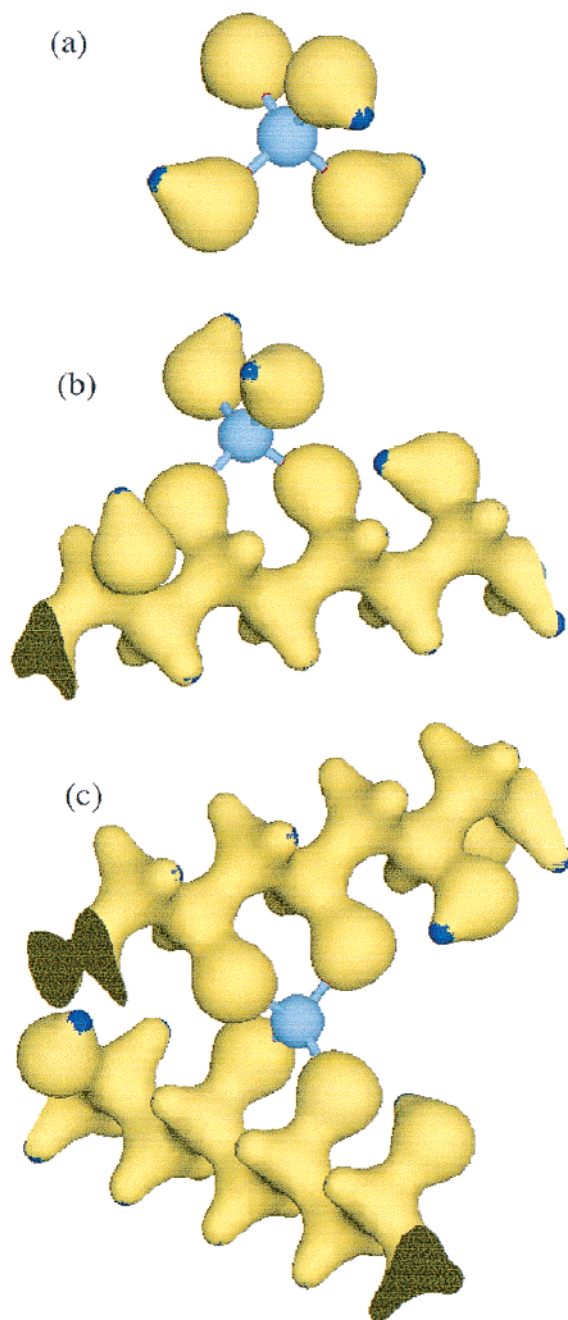
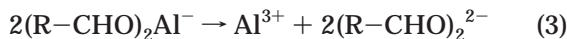
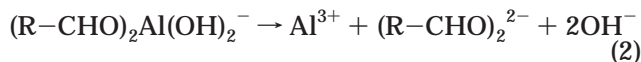
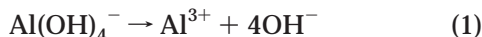


Figure 4. Isosurfaces of the valence electronic charge densities calculated for the different AlO_4 models investigated in the present study: (a) isosurface of the $\text{Al}(\text{OH})_4^-$ complex shown in Figure 3a; (b) isosurface of the Al–PVA(I) model shown in Figure 3b; (c) isosurface of the Al–PVA(II) model shown in Figure 3c. The isosurfaces correspond to an electron density of 0.14 e/au³.

turns out to be almost identical to that found for the $\text{Al}(\text{OH})_4^-$ complex. (It is worth noticing that the features of the charge density distributions are not affected by different choices of the value of the charge density sampled by a given isosurface.) In summary, the above geometries and charge density distributions show the formation of similar Al–O chemical bonds in the AlO_4 fragments of the three investigated systems. A first estimate of the stability of these Al–O bonds has been obtained by considering the following reactions of dissociation:

(34) *Lange's Handbook of Chemistry*; Dean J. A., Ed.; McGraw-Hill: New York, 1979.



where the reaction products are isolated ionic species. The above reactions are hypothetical ones because the Al–O bonds are broken by producing Al^{3+} and negative ions. Although these reactions have no experimental counterparts, they provide similar reaction products, thus allowing a comparison of the corresponding dissociation energies. These dissociation energies have been evaluated from differences between total energy values, e.g.:

$$D_1 = E[\text{Al}^{3+}] + 4E[\text{OH}^-] - E[\text{Al}(\text{OH})_4^-]$$

gives the dissociation energy for the reaction 1. In the following, it will be assumed that the dissociation energies relative to the above reactions, D_1 , D_2 , and D_3 in the order, give the fraction of dissociation energy corresponding to the breaking of one of the four Al–O bonds. Values of 15.4, 15.0, and 15.1 eV have been estimated for the D_1 , D_2 , and D_3 dissociation energies, respectively. These values are much larger than the value of 6.0 eV estimated for the dissociation energy of the diatomic Al–O molecule, which is not surprising because ionic species are formed in place of neutral ones. The closeness of the D_i values indicates that the stability of the Al–O bonds in the cross-linking configurations is comparable to that of the corresponding bonds in the stable $\text{Al}(\text{OH})_4^-$ complex. This result agrees with the similarities found for the geometry and the chemical bonding of the AlO_4 fragments in the Al–PVA and $\text{Al}(\text{OH})_4^-$ systems.

The energetics of the Al cross-linking has been also investigated by evaluating the energies released in the polycondensation reactions shown in Figure 2. These energies have been evaluated from the differences between the total energies of the involved species, that is

$$\Delta E_1 = E[(\text{R}-\text{CHO})_2\text{Al}(\text{OH})_2^-] + 2E[\text{H}_2\text{O}] - E[(\text{R}-\text{CHOH})_2] - E[\text{Al}(\text{OH})_4^-]$$

and

$$\Delta E_2 = E[(2(\text{R}-\text{CHO})_2)\text{Al}^-] + 4E[\text{H}_2\text{O}] - 2E[(\text{R}-\text{CHOH})_2] - E[\text{Al}(\text{OH})_4^-]$$

give the energies released in the reactions which lead to the configurations I and II of the Figure 2, respectively. The values calculated for ΔE_1 and ΔE_2 , -0.26 and -1.16 eV, respectively, clearly indicate that the formation of the Al–PVA(II) system is favored. Furthermore, they show that the ΔE_2 value—which is relative to the formation of four Al–O–C bonds—is much larger than twice that of ΔE_1 , which corresponds to the formation of two Al–O–C bonds. This result may be accounted for by considering the different distribution of the electronic charge in the ionic Al–PVA systems I and II (see parts b and c of Figure 4, respectively). Both

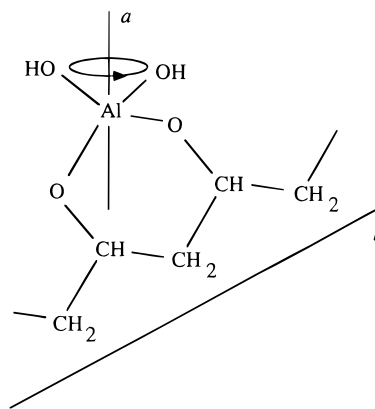


Figure 5. Schematic view of a rigid rotation, around the a axis, of the two OH groups bonded to the Al ion of the Al–PVA(I) model (see text and Figure 3b). All the other atoms in the model are fixed.

systems have an extra electronic charge. In the case of system I, this charge should be mainly localized on the oxygen atoms of the two OH groups bonded to Al. The O–H bonds have indeed a higher polarization than the O–C bonds involved in the formation of the Al–O–C bonds (see Figure 4b). In the case of the system II, in contrast, there is an uniform distribution of the extra electronic charge on the four, equivalent O atoms bonded with the Al atom, which is similar to that realized in the case of the $\text{Al}(\text{OH})_4^-$ complex (see parts a and c of Figure 4). The different delocalization of the electronic charge in systems I and II may account for the significant difference between the ΔE_1 and ΔE_2 values.

All the above results support the cross-linking of PVA chains by Al ions. It is worth noticing that similar AlO_4 atomic arrangements have been observed in organoaluminum compounds.^{35–37} Present results have been achieved by considering optimized molecular geometries in the absence of any external constraint. However, PVA chains embedded in the complex environment of a real MDF material may actually undergo structural distortions which have effects on the geometry of the AlO_4 fragment. To take into account those structural effects, the total energies of several distorted geometries of the Al–PVA(I) system have been calculated. More specifically, the two OH groups bonded with the Al atom have been rigidly rotated around the a axis in Figure 5 by keeping fixed all the other atoms. The rotation of the OH groups is measured by a rotation angle θ whose value $\theta = 0$ corresponds to the perfect tetrahedral configuration of the AlO_4 fragment. The total energy values of the Al–PVA(I) system corresponding to different values of θ are shown in Figure 6. The total energy of the distorted system has a smooth increase as the angle θ increases from 0 to 50° , and then it suddenly rises. This result indicates that Al cross-linking may be maintained even in the presence of appreciable structural deformations. Distorted geometries about a tetrahedrally coordinated Al atom have also been observed in the crystal structures of AlO_4 solid compounds.³⁸ It may be worth noticing that in the case of the Al–PVA(II) system, distortions, such as those simulated in the Al–PVA(I) system, do not involve hydrogen bonding between two PVA chains. The geometry shown in Figure 3c for the Al–PVA(II) system

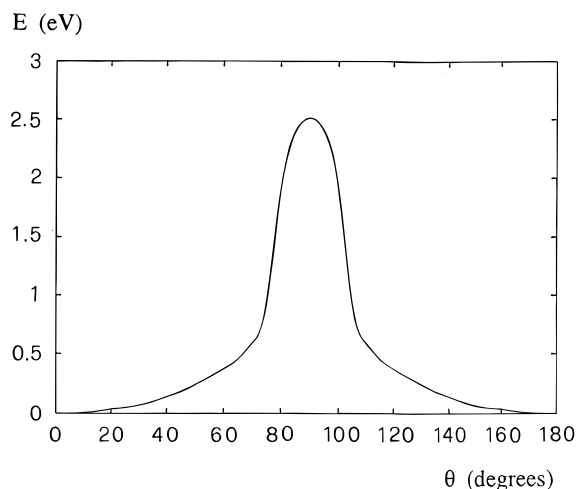


Figure 6. Profile of the total energy E of the Al-PVA(I) model (see text and Figure 3b), as a function of the angle θ measuring the rotation of the OH groups described in Figure 5. The value $\theta = 0$ corresponds to the perfect tetrahedral configuration of the AlO_4 fragment.

Table 2. Calculated and Experimental Values of Several Stretching Frequencies Relative to Chemical Bonds of the $2(\text{R-CHO})_2\text{Al}^-$ System (see the text)^a

bond	$2(\text{R-CHO})_2\text{Al}^-$	exp ^b
C-H	2870	2951
C-O(-H)	1098	1100
(C-)O-H	3627	3630
Al-O(-C)	848	

^a The vibrational frequencies are given in centimeters⁻¹. ^b Values from Ref. 41.

shows indeed that the involved PVA chains are aligned along two perpendicular directions. This geometry and the presence of the O-Al-O bonds lead to O-H distances close to 6 Å.

Finally, several vibrational frequencies have been investigated in the Al-PVA(II) system. The vibrational frequencies calculated for the C-H, C-O, and O-H bonds coincide with those obtained for an isolated PVA chain and are in good agreement with the experimental results (see Table 2). The frequency evaluated for the symmetric stretching mode relative to the four O atoms in the AlO_4 fragment, 848 cm^{-1} , has not been measured yet and deserves some attention. Raman spectra of solutions containing the $\text{Al}(\text{OH})_4^-$ complex exhibit a band at 621 cm^{-1} which is associated with the symmetric stretching mode of the AlO_4 group.³⁹ The same

stretching mode gives rise to a broad band at 1207 cm^{-1} in the Raman spectra of zunyite, an aluminosilicate mineral where an AlO_4 tetrahedron is surrounded by 12 octahedra formed by Al, O, and OH groups.⁴⁰

In the present case, the frequency calculated for the stretching mode of the AlO_4 fragment, 848 cm^{-1} , is midway between the vibrational frequency observed in the $\text{Al}(\text{OH})_4^-$ complex, where the OH groups may move outward without any constraint, and the frequency measured in zunyite, where the AlO_4 fragment is included in a rigid cage (in detail, the calculated frequency value is close to the mean value of the two measured frequencies, 914 cm^{-1}). Thus, if it is taken into account that the AlO_4 fragment investigated here is inserted in a "semirigid" framework formed by two PVA chains, the present estimate of the AlO_4 stretching mode appear to be quite reasonable. Moreover, the Al-O₄ stretching mode is Raman active and infrared inactive. This should favor the identification of this mode even in the presence of the vibrational frequencies observed within the range of 800–900 cm^{-1} in the infrared spectrum of PVA.¹⁷ The present theoretical estimate of the Al-O₄ stretching mode can be, therefore, very helpful to achieve an experimental evidence of cross-linking.

Conclusions

Present results give a strong support to the assumption that PVA chains are cross-linked by Al ions, thus indicating that Al plays a crucial role in the interaction between the inorganic and organic phases of the Al-based MDF materials. Furthermore, the O-Al-O bonds involved in the cross-linking seem strong enough to resist the effects of mechanical deformations of the PVA chains which likely occur in the MDF materials. The frequency of a symmetric stretching mode of the AlO_4 fragment involved in the PVA cross-linking has also been estimated. This Raman-active vibrational mode should favor the experimental identification of cross-linking. Finally, the present results give clear evidence of the relevance of the inorganic-organic interaction, thus suggesting further studies on the calcium-PVA interaction, which is concerned with the properties of the calcium-based MDF cements.

Acknowledgment. Thanks are due to Dr. Andrea Lapicciarella, to Dr. G. Guerrini (CTG Italcementi Group), and to Dr. G. Mattei for helpful discussion and comments.

CM990475T

(35) Atwood, D. A.; Rutherford, D. *Comments Inorg. Chem.* **1996**, 19, 25.

(36) Ziemkowska, W.; Pasykiewicz, S. *J. Organomet. Chem.* **1996**, 508, 243.

(37) Ziemkowska, W.; Pasykiewicz, S. *J. Organomet. Chem.* **1998**, 562, 3.

(38) Qijun, Y.; Sugita, S.; Xiuji, F.; Jinxiao, M. *Cem. Concr. Res.* **1997**, 27, 1439.

(39) Bartlett, J. R.; Cooney, R. P. *Spectroscopy of Inorganic-Based Materials*; Clark, R. J. H., Hester, R., Eds.; John Wiley: New York, 1987.

(40) Klopogge, J. T.; Frost, R. L. *Spectrochim. Acta* **1999**, 55A, 1505.

(41) Smith, L. A. *Applied Infrared Spectroscopy*; John Wiley: New York, 1979.